AMERICAN SOCIETY FOR MICROBIOLOGY | Antimicrobial Agents and Chemotherapy®

PHARMACOLOGY

Toward New Transmission-Blocking Combination Therapies: Pharmacokinetics of 10-Amino-Artemisinins and 11-Aza-Artemisinin and Comparison with Dihydroartemisinin and Artemether

Daniel J. Watson,[a] Lizahn Laing,[a] Liezl Gibhard,[b] Ho Ning Wong,[c] Richard K. Haynes,[c] Lubbe Wiesner[a]

[a]Division of Clinical Pharmacology, Department of Medicine, University of Cape Town, Cape Town, South Africa
[b]H3D, Department of Chemistry, University of Cape Town, Cape Town, South Africa
[c]Centre of Excellence for Pharmaceutical Sciences, Faculty of Health Sciences, North-West University, Potchefstroom, South Africa

ABSTRACT As artemisinin combination therapies (ACTs) are compromised by resistance, we are evaluating triple combination therapies (TACTs) comprising an amino-artemisinin, a redox drug, and a third drug with a different mode of action. Thus, here we briefly review efficacy data on artemisone, artemiside, other amino-artemisinins, and 11-aza-artemisinin and conduct absorption, distribution, and metabolism and excretion (ADME) profiling *in vitro* and pharmacokinetic (PK) profiling *in vivo* via intravenous (i.v.) and oral (p.o.) administration to mice. The sulfamide derivative has a notably long murine microsomal half-life ($t_{1/2}$ > 150 min), low intrinsic liver clearance and total plasma clearance rates (CL_{int} 189.4, CL_{tot} 32.2 ml/min/kg), and high relative bioavailability (F = 59%). Kinetics are somewhat similar for 11-aza-artemisinin ($t_{1/2}$ > 150 min, CL_{int} = 576.9, CL_{tot} = 75.0 ml/min/kg), although bioavailability is lower (F = 14%). In contrast, artemether is rapidly metabolized to dihydroartemisinin (DHA) ($t_{1/2}$ = 17.4 min) and eliminated (CL_{int} = 855.0, CL_{tot} = 119.7 ml/min/kg) and has low oral bioavailability (F) of 2%. While artemisone displays low $t_{1/2}$ of <10 min and high CL_{int} of 302.1, it displays a low CL_{tot} of 42.3 ml/min/kg and moderate bioavailability (F) of 32%. Its active metabolite M1 displays a much-improved $t_{1/2}$ of >150 min and a reduced CL_{int} of 37.4 ml/min/kg. Artemiside has $t_{1/2}$ of 12.4 min, CL_{int} of 673.9, and CL_{tot} of 129.7 ml/kg/min, likely a reflection of its surprisingly rapid metabolism to artemisone, reported here for the first time. DHA is not formed from any amino-artemisinin. Overall, the efficacy and PK data strongly support the development of selected amino-artemisinins as components of new TACTs.

KEYWORDS amino-artemisinins, pharmacokinetics, antimalarial agents, combination therapies, transmission-blocking

The efficacies of artemisinin combination therapies (ACTs) comprising one of dihydroartemisinin (DHA) 2, artemether 3, or artesunate 4 (Fig. 1) with piperaquine, mefloquine, amodiaquine, lumefantrine, or other are now being degraded in the face of increasing resistance of *Plasmodium falciparum* to the artemisinin component (1–3). Although initially reported in the countries of the greater Mekong subregion in Southeast Asia, evolution of resistant strains in other countries is now being reported (3–5). Resistance arises via induction of ring-stage quiescence in parasite phenotypes carrying point mutations, including C580Y in the *P. falciparum* Kelch 13 propeller domain (*Pf*K13) (6–11). It is held that DHA, used as a drug in its own right or as the principal metabolite of artemether and artesunate, competitively binds to *Pf*PI3K, which prevents the kinase binding to *Pf*K13. This thereby inhibits ubiquitinylation and proteasome degradation leading to cell cycle arrest and quiescence (12, 13). The problem is now compounded by decreasing efficacy of the ACT partner drug (2, 14–17). The response has been to extend the treatment regimen of the one ACT, to use two different ACTs in sequence (18, 19), or to conceptualize use of triple combination

Citation Watson DJ, Laing L, Gibhard L, Wong HN, Haynes RK, Wiesner L. 2021. Toward new transmission-blocking combination therapies: pharmacokinetics of 10-amino-artemisinins and 11-aza-artemisinin and comparison with dihydroartemisinin and artemether. Antimicrob Agents Chemother 65:e00990-21. https://doi.org/10.1128/AAC.00990-21.

Copyright © 2021 Watson et al. This is an open-access article distributed under the terms of the Creative Commons Attribution 4.0 International license.

Address correspondence to Richard K. Haynes, haynes@ust.hk, or Lubbe Wiesner, lubbe.wiesner@uct.ac.za.

Received 16 May 2021
Accepted 17 May 2021
Accepted manuscript posted online 7 June 2021
Published 16 July 2021

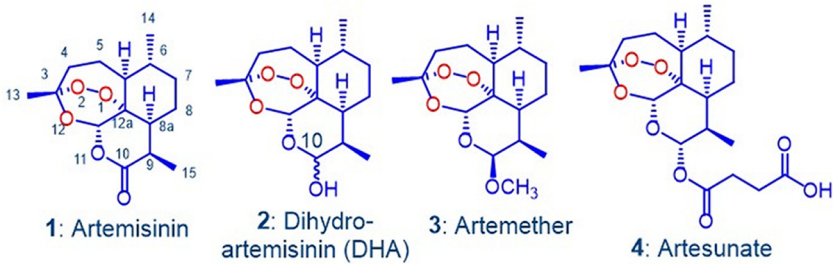

FIG 1 Artemisinin 1 and clinical derivatives DHA 2, artemether 3, and artesunate 4. The latter two are rapidly converted into DHA *in vivo* via metabolism or facile hydrolysis, respectively. As a hemiacetal, DHA rearranges irreversibly under physiological conditions into an active peroxyhemiacetal that in turn rearranges to the inert deoxyartemisinin (see references 41–44).

therapy (TACT) (14, 17). In the last case, DHA-piperaquine used with mefloquine or artemether-lumefantrine with amodiaquine in clinical trials indeed resulted in enhanced efficacy; for the DHA-piperaquine-mefloquine regimen, efficacy was improved from 48% for the ACT to 98% for the TACT (20). However, use of such TACTs (as is the case with current ACTs) involving the current clinical artemisinins combined with known drugs without any regard to intrinsic mechanism (21) or pharmacodynamic or pharmacokinetic aspects also carries the risk of amplifying resistance (22, 23). Also, mass drug administration (MDA) programs using ACTs to clear subclinical reservoirs of resistant parasites in Southeast Asia are under way. Thus, administration of 3-day courses of DHA-piperaquine plus single dose primaquine each month for 3 months to village populations in Cambodia is being carried out (24, 25). The practice has been criticized on ethical grounds, ambiguity in definition of subclinical parasites, and use of substantial resources in the face of outcomes that are not easily defined (26–28). Irrespective of these issues, the abnormally protracted treatment and MDA regimens do require increased pharmacovigilance (29). Nevertheless, other control modalities, including enhanced surveillance, reliable detection and treatment of infected individuals from urban, agricultural, or remote forested areas, use of insecticide-treated bednets, vector control, etc., are enhancing progress toward the goal of achieving malaria elimination in the greater Mekong subregion (30).

The artemisinins in the current ACTs (Fig. 1) have been in use since their introduction by the Chinese in the 1970s and 1980s (31–33). These, including DHA, are inducers of their own metabolism (34–36) and elicit neurotoxicity concerns (29, 37–40). DHA is thermally unstable and in aqueous solution readily rearranges to a peroxyhemiacetal (41–45) whose formation also may intrude during preparation and storage of DHA (45). Such properties highlight the intemperance associated with development of DHA as an antimalarial drug (42, 43, 46). Overall, new therapies involving rational combinations of novel drugs are urgently required for treatment of multidrug-resistant malaria (23). To this end, we are developing combinations based on discrete consideration of mechanism of action of the components (47, 48). For the first drug, we focus on new artemisinin derivatives that have enhanced efficacies against all blood stages of the malaria parasite and ideally retain baseline activities against artemisinin-resistant strains. The rationale and data supporting use of a redox-active second drug such as methylene blue which displays synergism with the new artemisinins (47, 48) and a third drug type such as a quinolone (49) based on a distinct target are presented in detail elsewhere. The artemisinin derivatives bear an amino group attached to C-10 (44) wherein antimalarial activity is enhanced (50). Examples are given in Fig. 2; these are structurally distinct to the artemisinins of Fig. 1 bearing an oxygen-linked substituent at C-10.

The best known amino-artemisinin is artemisone 6 (Fig. 2) (51, 52). It is nonneurotoxic (51, 53) and does not induce its own metabolism (54). The principal metabolite M1 12 (Fig. 2) is formed together with other metabolites structurally related to artemisone and M1 bearing hydroxyl groups at C-5 and C-7, all of which retain antimalarial activity (51, 54). Artemisone is active against murine cerebral malaria; treatment at prescribed low dose levels were

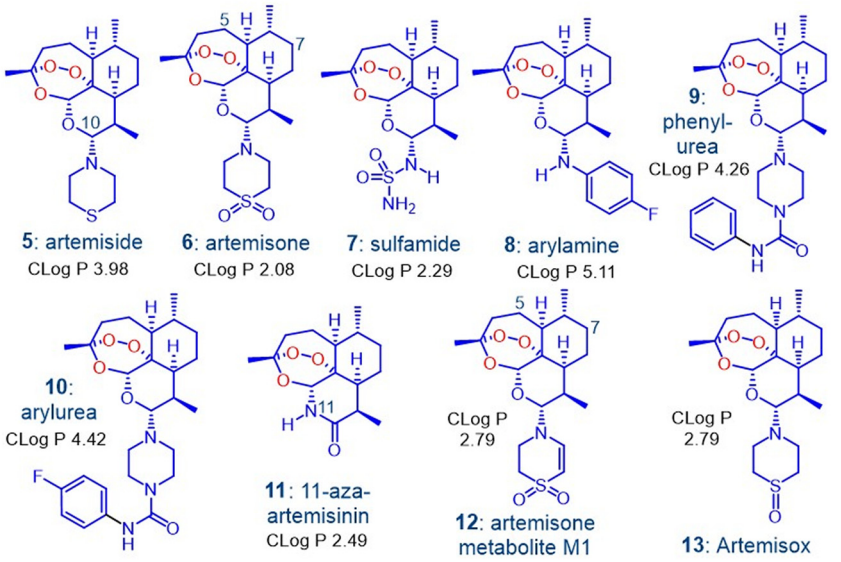

FIG 2 The amino-artemisinins 5 to 10 in which the exocyclic oxygen atom at C-10 of the clinical artemisinins (Fig. 1) is replaced by a nitrogen atom and 11-aza-artemisinin 11 in which an –NH group replaces O-11. As discussed below, artemiside 5 is rapidly metabolized to artemisone 6, which must proceed via artemisox 13, and then to M1 12, the primary metabolite of artemisone. Calculated log *P* data are given, and efficacy data for 1 to 12 appear in references 47, 48, and 61–63 and are summarized in Tables S1 to S7.

completely curative, whereas at the same dose levels, DHA and artesunate, the latter of which is currently used for treatment of cerebral malaria, elicited no cure (55). In a phase IIa trial of patients with nonsevere malaria, artemisone was curative at one-third the dose level of artesunate (54, 56–59). With this earlier data serving as a backdrop to our current efforts, we needed to establish if other amino-artemisinins possess efficacy and drug metabolism and pharmacokinetic (DMPK) profiles superior to those of artemisone 6. Thus, we conducted efficacy screens on artemiside 5, the sulfide precursor of artemisone 6 (51, 52), on artemisone 6 itself as comparator, the 10-sulfamide 7 (51), the 10-(*p*-fluorophenyl)amino derivative 8 (60), the 10-(phenylpiperazine)- and 10-(*p*-fluorophenylpiperazine) urea derivatives 9 (47) and 10 (48), 11-aza-artemisinin 11 (61, 62), and the metabolite M1 (63) 12 (Fig. 2). Several were screened against asexual blood stages of artemisinin-resistant *P. falciparum* clones ARC08-22 (4G) and PL08-009 (5C) carrying the *Pf*KI3 C580Y mutation (64) and also against liver-stage *P. berghei* (*Pb*) sporozoites (48). The data are summarized in Tables S1 to S7 in the supplemental material.

Salient features are as follows. Artemiside, artemisone, and the arylurea possess 50% inhibitory concentration (IC_{50}) activities ranging from 0.85 to 1.75 nM against asexual blood stages of CQ-sensitive *Pf*NF54 and multidrug-resistant K1 and W2 strains. The sulfamide, arylamine, and phenylurea are slightly less active against all strains (1.3 to 4.7 nM), and 11-aza-artemisinin is the least active (6.02 to 10.48 nM) (Table S2) (62). Cytotoxicity assays, including those against Chinese hamster ovary (CHO) cells, indicate that the arylamine and phenylurea (50% effective concentration [EC_{50}] 2.4 to 2.9 μM) are more toxic than artemiside, artemisone, and the arylurea (204 to >271 μM) (Table S1) (47, 48). The amino-artemisinins are active against blood-stage *P. falciparum* gametocytes, with activities (IC_{50}) against early-stage gametocytes (EG > 90% stage I to III) ranging from 1.94 nM for artemisone to 83 nM for the phenylurea. Against late-stage gametocytes (LG > 90% stage IV and V), the sulfamide is the least active (IC_{50} 419.4 nM), with activities of the other compounds ranging from 1.5 to 42.4 nM. Thus, the latter are appreciably more active than methylene blue, a known gametocytocidal agent (65), with EG IC_{50} of 95 nM and LG of 143 nM (Table S3). These activities thus portend utility of the amino-artemisinins as transmission-blocking agents (47, 48). 11-Aza-artemisinin is less active with EG IC_{50} of 170.4 and LG of 166.1 nM (Table S4) (62). Against liver-stage *P. berghei* sporozoites, IC_{50} values range from 28.3 nM for

TABLE 1 Solubilities, microsomal stabilities, and plasma protein binding of the artemisinins[a]

	Solubility (μM)[b]			Microsomal half-life $t_{1/2}$ (min)			Intrinsic liver clearance rate CL_{int} (ml/min/kg)			Hepatic extraction ratio E_H			
Compound	pH 2	FaSSIF pH 6.5[c]	pH 7.4	Mouse	Rat	Human	Mouse	Rat	Human	Mouse	Rat	Human	Plasma protein binding f_u
DHA 2	<5[d]	<5[d]	<5[d]	135.9	90.0	51.7	50.2	34.7	41.5	0.4	0.4	0.7	ND[e]
Artemether 3	ND	ND	ND	17.4	<10	12.5	392.8	988.2	171.7	0.8	0.9	0.9	0.14
Artemiside 5	12.4	<5	<5	12.4	<10	<10	551.3	1,389.2	450.8	0.9	1.0	1.0	0.23
Artemisone 6	73.7	74.4	120.4	<10	<10	<10	805.2	342.5	242.6	0.9	0.9	0.9	0.14
Sulfamide 7	>150	<5	11.5	>150	94.9	>150	41.3	32.9	5.6	0.3	0.4	0.2	0.17
Phenylurea 9	75.6	<5	<5	13.5	<10	<10	506.0	1,539.0	394.5	1.7	1.0	ND	0.14
Arylurea 10	10.0	24.0	27.0	<10	ND	<10	2,485.0	ND	531.0	0.6	ND	0.6	0.02
11-Aza-artemisinin 11	>150[f]	>150[f]	144.2[f]	>150	>150	60.0	36.4	9.0	ND	0.3	0.1	ND	0.13
M1 12	>150	57.6	74.5	>150	28.8	>150	37.4	108.5	ND	0.3	0.7	ND	0.25

[a]Each value was obtained as technical triplicates, $n = 3$; ND, not determined.
[b]Kinetic solubility was determined in three solutions at a concentration of 200 μM but at different pH values which represent that of the gastrointestinal tract.
[c]FaSSIF buffer mimics the fasted state (87).
[d]Solubility of DHA could not be determined in the buffer solutions because of decomposition.
[e]Plasma protein binding could not be calculated as DHA was unstable in plasma.
[f]11-Aza-artemisinin did not readily dissolve in DMSO, and therefore the calibration standards used in this experiment were prepared in methanol.

artemisone to 81.3 for artemiside to 105.5 nM for the arylurea (Table S5); in comparison, artemether has an IC_{50} of $>10^4$ nM (48). Against asexual blood stages of artemisinin-resistant clones carrying the *Pf*KI3 C580Y mutation, artemiside and artemisone (IC_{50} W2 equal to 1.69 to 2.21 nM) are equipotent against clone ARC08-22 (4G) (1.62 to 2.43 nM) and more active against the PL08-009 (5C) clone (0.27 to 0.29 nM). The phenylurea is also active against the ARC08-22 (4G) clone. DHA elicits activities of 6.41 to 6.68 nM against these clones (Table S6) (48). The retention of efficacy of artemisone against artemisinin-resistant clones is consistent with earlier results involving Cambodian *P. falciparum* wild-type (WT) isolates transfected to strains CamWTC580Y (C580Y K13 mutation), Cam3.IIC580Y (C580Y K13), and Cam3.IIRev (wild-type K13 sequence), wherein it essentially retains baseline activities across all strains, as reflected in a mean IC_{50} 2.4 nM (66); activity against W2 is 1.9 nM. For DHA, activities are 11.2 and 5.2 nM, respectively. The metabolite M1 is active against drug-sensitive and- resistant strains of *P. falciparum* (IC_{50} 2.5 to 8.6 nM) but less so than artemisone (IC_{50} 0.7 to 1.1 nM) (63). However, artemisone and M1 do induce quiescence in W2 ring-stage parasites but not in a concentration-dependent manner; cultures treated with different concentrations of these drugs reach 1% parasitemia within the same time period (63). Work is under way probing the basis of this effect and how these and other drugs to be used in the putative combinations may modulate induction of quiescence in ring-stage assays involving the resistant phenotypes or indeed kill the quiescent rings.

Overall, artemiside, artemisone, and the arylurea are the frontrunners in terms of global efficacies and relatively low toxicities *in vitro*. However, expression of therapeutic efficacy depends not only on biological activity but also on pharmacokinetic (PK) properties. This becomes important for the envisaged drug combinations (67). We report here on the *in vitro* absorption, distribution, metabolism, and excretion (ADME) properties and PK measurement in a murine model of the compounds of Fig. 2. Initially, the arylamine 8 was also included, but preliminary PK assessment in the murine model unexpectedly indicated untoward toxicity, so it was not further examined. The data are directly compared to those of DHA and artemether. An evaluation of the compounds to be taken forward is then presented.

RESULTS

ADME profiling *in vitro*. The kinetic solubilities, plasma protein binding, metabolic stability, and calculated intrinsic clearance rates and hepatic extraction ratio E_H for mouse, rat, and human liver microsomes (68) are shown in Table 1.

It was not possible to measure solubility of DHA at any pH because of decomposition, as noted previously (44, 51). DHA presented high clearance rates in all three microsomal systems, and again in accord with previous observations (43), the extent of plasma protein

binding could not be established due to decomposition. The aqueous solubility of artemether was not able to be determined here but is variously recorded to be $<$1 mg/ml, 12.1 mg/liter at 25°C (69), 0.3 mg/ml (70), or rated as insoluble (71). It also displayed poor metabolic stability with high clearance rates with mouse (MLM), rat (RLM), and human liver microsomes (HLM). This lability coupled with its auto-induction of metabolism is already established (34, 35). The relatively lipophilic artemiside with log *P* of 4.97 and calculated log *P* (ClogP) of 3.98 (Fig. 2) has low aqueous solubility of $<$2 mg/liter or $<$5.4 μM at pH 7.2 (51). Here, the compound displayed low aqueous solubility in the FaSSIF buffer at pH 6.5 and phosphate-buffered saline (PBS) buffer at pH 7.4. This suggests that it would be absorbed poorly in the fasted state. At pH 2, the modest increase in solubility to 12.4 μM is ascribed to formation of the more polar conjugate acid, with a calculated pK_a of 6.99, arising from protonation of the nitrogen atom of the thiomorpholine ring. Notably, artemiside displayed high intrinsic clearance rates and short half-lives in all three liver microsome systems, predominantly due to its facile metabolism to artemisone as described below. It displayed hepatic extraction ratios in all three systems comparable to those of artemether, again suggesting it would be rapidly metabolized in the liver. The more polar artemisone (log *P* of 2.49, ClogP of 2.08, aqueous solubility at pH 7.2 of 89 mg/liter or 221.6 μM) (51) was appreciably more soluble in the aqueous buffers but displayed high clearance rates and low half-lives in all three liver microsome systems. The artemisone metabolite M1, ClogP 2.79, displayed solubility in the three aqueous buffers on par with that of artemisone but in notable contrast displayed greatly improved half-lives in the liver microsome systems. Interestingly, it exhibited varied metabolic stabilities in the different microsome systems, displaying a moderate clearance rate in MLM, a high clearance rate in RLM, and a very low rate in HLM. The sulfamide 7 is less polar (logP of 3.36, ClogP of 2.29) (51) than artemisone and was reported to possesses good solubility in water at pH 7.2 (294 mg/liter or 811 μM) (51). However, here, while it displayed acceptable solubility at pH 2, it exhibited poor solubility in the other aqueous buffers. It was cleared at a moderate rate by MLM and RLM, although comparatively it had an encouragingly low clearance rate in HLM, indicative of a less facile metabolism. The phenylurea 9 had improved solubility at pH 2 only but displayed very high clearance rates and low half-lives. The arylurea 10 exhibited moderate solubility in all three aqueous buffers and was cleared rapidly in MLM and HLM. 11-Aza-artemisinin 11 displayed the best solubility of all compounds ($>$144.2 μM) in the three aqueous solutions; as it contains no basic nitrogen atoms, this represents an intrinsic solubility. It also displayed the lowest clearance rates in all three microsome systems with a moderate clearance rate in MLM and a low rate in RLM. Notably, the half-life, clearance rate, and extraction ratio of 11-aza-artemisinin could not be calculated in HLM as it was found to be stable throughout the experiment. This represents the first determination of the metabolic stability of this well-known compound.

The artemisinins presented moderate plasma protein binding as reflected in the unbound fraction ranging from 0.13 to 0.25. The one exception is provided by the arylurea 10, which had the highest plasma protein binding as reflected in the fraction unbound (f_u) of 0.02.

Pharmacokinetic properties in mice. PK properties were determined in healthy male C57BL/6 mice by intravenous (i.v.) (Table 2) and oral (p.o.) administration (Table 3). Calibration curves were used to determine the drug concentrations *in vivo* of the artemisinins from mouse plasma. The calibration curves fitted quadratic regressions over the range of 3.9×10^{-3} μg/ml to 4.0 μg/ml for artemether, artemiside, artemisone, the arylurea, and 11-aza-artemisinin and 1×10^{-3} μg/ml to 4.0 μg/ml for the sulfamide and phenylurea. The accuracy (percentage nominal concentration [Nom]) and precision (percentage of coefficient of variation [CV]) statistics of the low-, medium-, and high-quality controls for artemether, artemiside, the phenylurea, arylurea, and 11-aza-artemisinin were between 72.2 to 125.9% and 0.2 to 11.8%, respectively, and were 71.2% to 111.1% and 0.7 to 14.5% for artemisone and sulfamide, respectively, during sample analysis. Tafenoquine is an 8-aminoquinoline and is prescribed for prophylaxis and treatment of *P. vivax* infections (72). The PK data of tafenoquine recorded using

TABLE 2 Pharmacokinetic parameters calculated from the intravenous administration (i.v.) of the artemisinins to male C57/BL6 mice at a dose of 10 mg/kg ($n = 3$)[a]

Compound (i.v.)	$t_{1/2}$ (h)	V (liter/kg)	CL_{tot} (ml/min/kg)	CL_{int} (ml/min/kg)	AUC (min/μmol/liter)
Artemether 3	1.4 ± 0.2	14.1 ± 1.3	119.7 ± 39.0	855.0	304.4 ± 80
DHA 2 from i.v. artemether 3					155 ± 17
Artemiside 5	1.8 ± 0.5	24.3 ± 9.3	155.0 ± 46.4	673.9	184.9 ± 43
Artemisone 6 from artemiside 5					28.9 ± 1
M1 12 from artemiside 5					13.8 ± 9
Artemisone 6	0.5 ± 0.03	1.9 ± 0.1	42.3 ± 2.1	302.1	577.5 ± 30
M1 12 from artemisone					60.6 ± 36
Sulfamide 7	0.6 ± 0.1	1.63 ± 0.4	32.2 ± 6.2	189.4	864.1 ± 213
Phenylurea 9	1.3 ± 0.1	6.03 ± 0.3	55.9 ± 3.3	399.3	431.9 ± 27
Arylurea 10	1.3 ± 0.3	6.92 ± 2.9	58.9 ± 3.5	2,945.0	315.9 ± 33
11-Aza-artemisinin 11	3.1 ± 0.8	19.4 ± 7.5	75.0 ± 8.9	576.9	462.7 ± 117
Tafenoquine[b]	43.7 ± 1.5	2.34 ± 0.0	ND	1.84	2,363 ± 146

[a]CL_{tot}, total plasma clearance; CL_{int}, intrinsic plasma clearance; V, volume of distribution during elimination phase; AUC, area under the concentration-time curve from 0 h to last; ND, not determined. Mean ± standard deviation (SD) reported.
[b]Data from reference 73.

the murine model described here (73) are included in Tables 2 and 3. It demonstrates a very long half-life, a low intrinsic clearance rate, and a relatively high bioavailability. The properties stand in stark contrast to those of the artemisinins and highlight the notably poor "drug-likeness" (74) of the latter.

The plasma concentration-time curves derived from the PK data are shown in Fig. 3 to 7. Artemether (Fig. 3) exhibited a short half-life (1.4 h) with a high intrinsic clearance rate (855.0 ml/min/kg) and a low bioavailability of 2%. DHA was rapidly formed following i.v. and p.o. dosing (Fig. 3). This underscores the lability of artemether as noted elsewhere (34, 35).

Artemiside displayed a short half-life (1.8 h) as well as a high clearance rate (673.9 ml/min/kg) and a low bioavailability of 1%. Notably, we record here for the first time that it was relatively rapidly metabolized to artemisone and subsequently into the unsaturated metabolite M1 (Fig. 4). Artemisone had the shortest half-life (0.5 h) and a high intrinsic clearance rate (302.1 ml/min/kg), which matches the calculated *in vitro* ADME data (Table 1). Despite this, artemisone displayed PK parameters that were improved relative to those of the other artemisinins (Table 2). It was rapidly converted into the metabolite M1 following an oral dose of 50 mg/kg (Fig. 5) and possessed an improved bioavailability of 32%. This compares quite well with earlier data obtained following a single oral dose of artemisone at each of 3, 10, and 30 mg/kg to female rats (51, 54). Thus, peak plasma concentrations were reached between 15 and 60 min. The corresponding C_{max} and elimination half-lives were 35, 230, and

TABLE 3 Pharmacokinetic parameters calculated from the oral administration (p.o.) of the artemisinins to male C57/BL6 mice at a dose of 50 mg/kg ($n = 3$)[a]

Compound (p.o.)	T_{max} (h)	C_{max} (μM)	AUC (min/μmol/liter)	F (%)	Ratio $AUC_{(0-last)}$ metabolite/parent
Artemether 3	0.1 ± 0.0	0.6 ± 0.2	32.3 ± 20	2 ± 0.6	
DHA 2 from artemether 3			77 ± 12		1.9
Artemiside 5	1.0 ± 0.9	0.1 ± 0.01	9.5 ± 2.5	1 ± 0.2	
Artemisone 6 from artemiside 5	1.3 ± 0.8	0.8 ± 0.3	101.5 ± 49		9
M1 12 from artemiside 5	0.3 ± 0.0	0.1 ± 0.02	20.8 ± 8		1.4
Artemisone 6	0.3 ± 0.1	8.0 ± 0.8	922.7 ± 348	34 ± 7.5	
M1 12 from artemisone 6	0.1 ± 0.1	2.1 ± 0.3	173.3 ± 51.7		0.2
Sulfamide 7	0.6 ± 0.2	21.7 ± 1.2	2,562.3 ± 499	59.3 ± 11.6	
Phenylurea 9	0.5 ± 0.0	1.0 ± 0.1	149.5 ± 5.9	6.9 ± 0.3	
Arylurea 10	0.5 ± 0.0	2.3 ± 0.3	276.5 ± 48.4	17.5 ± 3.1	
11-Aza-artemisinin 11	0.5 ± 0.0	2.6 ± 0.01	154.9 ± 10	7.15 ± 0.3	
Tafenoquine[b]	9.0 ± 1.0	3.06 ± 0.37	11,368 ± 1,232	55 ± 2	NA

[a]C_{max}, maximum concentration; T_{max}, time to C_{max}; AUC_{0-last}, area under the concentration-time curve from 0 h to last; F, oral bioavailability; NA, not applicable. Mean ± SD reported.
[b]Data from reference 73.

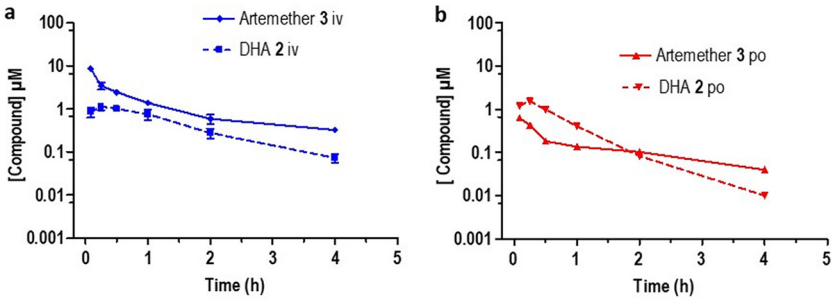

FIG 3 Plasma concentration-time curves for artemether 3 (solid line) and its metabolite DHA 2 formed following (a) intravenous dosing (i.v.) and (b) oral dosing (p.o.). All results are presented as the mean ± standard deviation.

850 μg/liter and 0.18, 0.37, and 0.54 h. Based on intravenous AUC data, the bioavailability of artemisone ranged from 5 to 25%, in rough agreement with that observed here. Also noted earlier was an apparent facile saturation of first pass metabolism based on 4-week toxicological studies in female rats. Importantly, the measured $t_{1/2}$ of artemisone in rats was at marked variance with the data obtained from *ex vivo* bioassay studies which suggest that $t_{1/2}$ in a primate model is about 2 to 3 h (51). This was also confirmed by *ex vivo* bioassay of human plasma samples taken during phase I studies (54). Thus, bioassay of subject plasma samples showed artemisone equivalent concentrations to be about 2.3-fold higher at T_{max} than that measured by liquid chromatography-tandem mass spectrometry (LC/MS-MS) for artemisone. The discrepancy arises because the *ex vivo* bioassay screen measures total activity of artemisone plus the active metabolite M1 and the hydroxylated counterparts in monkey or human plasma.

The sulfamide showed a short half-life (0.6 h) following i.v. or p.o. dosing but revealed promising exposure levels with a bioavailability of 59% (Fig. 6a). It exhibited an intrinsic clearance rate (189.4 ml/min/kg) which was the lowest of the artemisinins evaluated here. 11-Aza-artemisinin (Fig. 6b) displayed the longest half-life (3.1 h) but had a high intrinsic clearance rate (576.9 ml/min/kg) and an oral bioavailability of 7%. This does not correlate with the calculated *in vitro* ADME data which suggest that it is notably stable with a low intrinsic clearance rate (Table 1). The phenylurea 9 (Fig. 7a) had a poor exposure, resulting in a low bioavailability of 6.9%. It also had a short half-life (1.3 h) and a high intrinsic clearance rate (399.3 ml/min/kg). Notably, the arylurea 10 (Fig. 7b), differing from the phenylurea in possessing a fluorine atom at C-4 of the phenyl ring (Fig. 2), presented parameters similar to those of arylurea 9 in possessing a short half-life (1.3 h), a notably rapid clearance (2,945.0 ml/min/kg), and bioavailability of 17.5%.

Importantly, DHA was not detected as a metabolite of either artemiside or artemisone (the latter in accord with previously reported data [51, 54]), the sulfamide, 11-aza-artemisinin, or the phenyl and aryl ureas. The facile metabolism of artemiside to artemisone and thence the metabolite M1 is noteworthy.

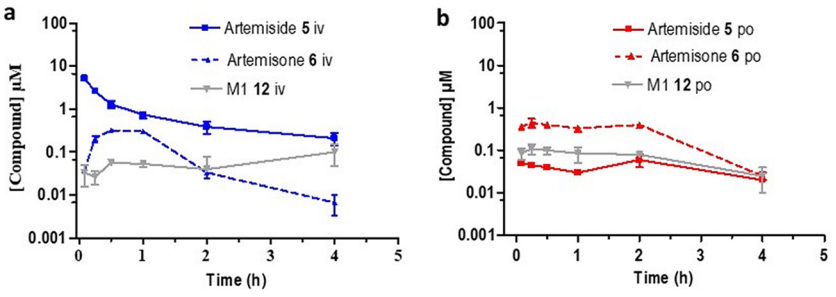

FIG 4 Plasma concentration-time curves for artemiside 5 (solid line) and its metabolites artemisone 6 (dashed line) and M1 12 (solid gray line) formed following (a) intravenous dosing (i.v.) and (b) oral dosing (p.o.). All results are presented as the mean ± standard deviation.

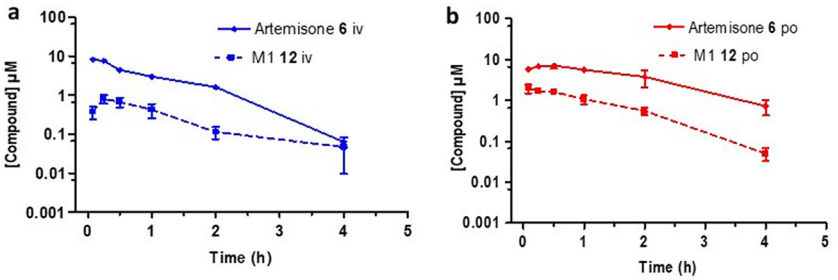

FIG 5 Plasma concentration-time curves for artemisone 6 (solid line) and its metabolite M1 12 (dashed line) formed following (a) intravenous (i.v.) and (b) oral (p.o.) dosing. All results are presented as the mean ± standard deviation.

DISCUSSION

The data overall highlight the problems of metabolic stability, poor solubility, and short half-lives of the artemisinins at large. In addition, a comparison with the far more stable and better absorbed tafenoquine emphasizes the lack of drug-likeness and difficulties in applying drug-design precepts to artemisinins (74, 75). However, in comparison with DHA and artemether, the amino-artemisinins do elicit more favorable properties, although within this series in particular, the differences do not enable a clear-cut decision to be made on the "best" amino-artemisinin, with several possible exceptions. Further, any "stop-go" criteria must also incorporate overall cost of production of a particular candidate and especially relative lack of toxicity coupled with efficacy against all stages of the malaria parasite.

The inability to measure the kinetic solubility of DHA or to assess the extent of plasma protein binding because of decomposition reflects its instability (43, 45, 46, 51). However, it was possible to measure clearance rates in the microsomal systems, and these were among the slowest of the artemisinins (Table 1). Artemether displayed low exposure levels as measured by AUC values (Table 3), which is likely due to rapid plasma clearance when administered intravenously. The low bioavailability of artemether (Table 3) reflects its poor absorption and limited systemic exposure. As previously recorded (34, 35), it is rapidly metabolized to DHA; indeed, the transformation is so rapid that artemether is considered a prodrug for DHA (75).

For the first amino-artemisinin artemiside, the PK data resemble those of artemether in terms of rapid plasma clearance and volumes of distribution. The exposure and bioavailability are limited by low aqueous solubility, but they are notably susceptible to microsomal biotransformation (Table 1; Fig. 4) via rapid oxidative conversion of the thiomorpholine sulfide to the sulfone of artemisone. Such a facile sulfide to sulfone biotransformation must proceed via the known sulfoxide artemisox (51) (Fig. 2). An analogous transformation has been mapped out for the anthelmintic drug albendazole incorporating a propylthio group attached to a benzimidazole. This undergoes rapid first pass metabolism via oxidation of the sulfide to the bioactive

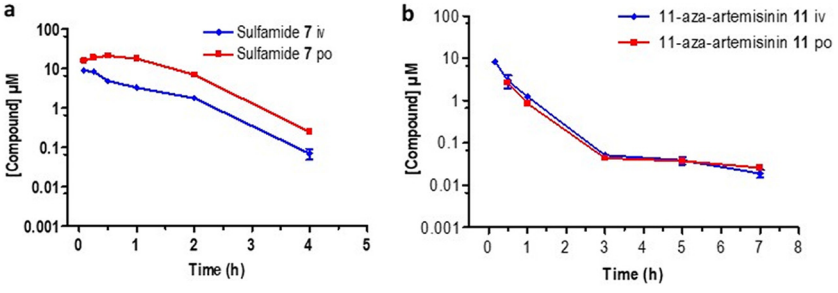

FIG 6 Plasma concentration-time curves for (a) sulfamide 7 and (b) 11-aza-artemisinin 11 following intravenous (i.v., blue line) and oral (p.o., red line) dosing. All results are presented as the mean ± standard deviation.

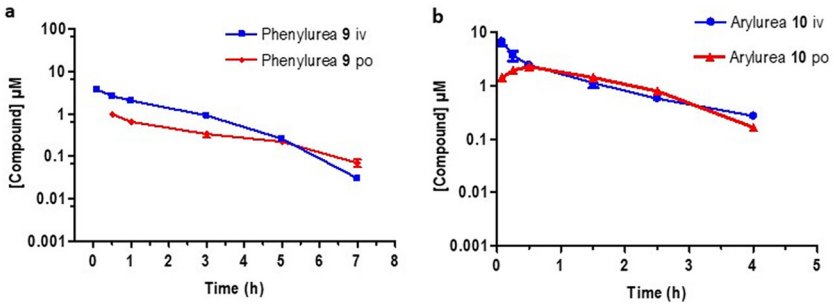

FIG 7 Plasma concentration-time curves for (a) the phenylurea 9 and (b) the arylurea 10 following intravenous (i.v., blue line) and oral (p.o., red line) dosing. All results are presented as the mean ± standard deviation.

sulfoxide and then to the sulfone (76). Likewise, metabolism of the antitrypanosomial drug fexinidazole carrying a (4-methylthio)phenoxyl group attached to a nitroimidazole proceeds via way of the corresponding sulfoxide to the sulfone, both more polar metabolites that in contrast to fexinidazole itself elicit blood concentrations above their effective therapeutic doses against the nonapicomplexan parasite *Leishmania donovani* (77, 78). Thus, while the "prodrug" concept may be applied here to artemiside, the drug is highly active in its own right *in vitro* against *P. falciparum* (Tables S1 and S3). Also, the AUC of artemisone generated *in situ* following oral dosing of artemiside was 9-fold lower than the exposure level achieved upon oral dosing of artemisone itself (Table 3). While this initially suggests that dosing of artemiside does not result in higher levels of artemisone, no account is made here for formation and biotransformation rate of the intermediate artemisox. These aspects, including efficacy data for artemisox, the ramifications for its formation during metabolism of artemiside, and overall effects on bioavailability and plasma levels, are discussed separately.

Artemisone showed PK properties superior to those of artemether. While it possesses a low elimination half-life (Table 2), it has a much higher oral bioavailability (Table 3), reflecting more efficient absorption and slower clearance. These results correlate well with the microsomal stability (Table 1). Improved absorption may be attributed to improved solubility at physiological pH. Artemisone forms the active metabolite M1 bearing unsaturation in the thiomorpholine *S,S*-dioxide ring. This metabolite and its hydroxylated derivatives substantially add to overall efficacy of artemisone according to *ex vivo* bioassays of monkey plasma (51, 54). Metabolite M1 elicits solubility in aqueous solutions at the different pH values on par with that of artemisone but, in contrast, possesses substantially greater microsomal half-lives (Table 1). Thus, in comparison to the DHA metabolite formed from artemether or artesunate, M1 is more soluble, is more stable, and possesses excellent *in vitro* activities against asexual blood stages of sensitive and multidrug-resistant *P. falciparum* (see Table S7 in the supplemental material) (63). From a chemical viewpoint, it is noted that while *N*-dealkylation of drugs incorporating six-membered cyclic tertiary amines appears to be the characteristic pathway for metabolism (79, 80), desaturation as observed here is decidedly less prevalent.

The sulfamide showed PK properties that were significantly improved compared to those of artemether, including greatly improved overall systemic exposure, represented by a greater C_{max} and a distinctly higher bioavailability (Table 3). Interestingly, the sulfamide had a low volume of distribution and a low clearance rate, which suggest low tissue penetration. The microsomal stability assays suggest that it is not as susceptible to biotransformation as are the other compounds (Tables 2 and 3). It is noted that analogues of the sulfamide have been prepared carrying piperazine-pyridyl substituents (48), and although efficacies are marginally improved, the additional synthetic chemistry efforts cannot now be justified in the face of the accessibility of the sulfamide (51) and its relatively favorable PK profile noted here.

With respect to the phenyl and aryl ureas (Fig. 2), we prepared the latter on the basis that the *p*-fluorine atom would block oxidation of the phenyl ring via arene oxide formation

during phase I metabolism, thereby rendering the compound less toxic *in vivo*. Strikingly, however, the arylurea is substantially less toxic *in vitro* against mammalian cell lines, including CHO cells, than is the phenylurea (CHO EC_{50} of 204 μM versus 2.4 μM; Table S1) (48). The arylurea also has solubility that is improved relative to that of the phenylurea at higher pH (Table 1), and both compounds show relatively good bioavailability compared to that of artemether, although it is inferior to that of artemisone (Table 3). The compounds, like artemisone, are rapidly absorbed, as indicated by the respective T_{max} values (Table 3).

11-Aza-artemisinin displayed a short half-life following intravenous administration (Table 2), which appears to be contrary to the calculated clearance *in vitro* (Table 1). When administered orally, it was poorly absorbed (Table 3). The compound possesses a secondary amide group that is an efficient H-bond donor-acceptor ensemble (81). Thus, the H-bonding capacity may explain poor absorption *in vivo*; it may not be able to pass via passive diffusion through cell walls. 11-Aza-artemisinin is at a higher oxidation state than is DHA, so it is unable to be metabolized into DHA (82); indeed, the metabolite could not be detected here. While its greatly enhanced thermal and hydrolytic stability with respect to those of other artemisinins have been demonstrated (61), the relative stability evinced here, albeit in *in vitro* screens using microsomes, is encouraging. This well-known compound is prepared in one economic step from artemisinin (61, 82), but it displays relatively mediocre activity *in vitro* against *P. falciparum*.

New antimalarial compounds should meet one or more target compound profiles (TCP) in order to inhibit the malaria parasite at different stages of its life cycle and thus relieve clinical symptoms, avoid relapse, and block transmission (83). The amino-artemisinins possess potent activities *in vitro* against asexual blood stages of drug-sensitive and -resistant *P. falciparum* strains, and selected compounds display activities against transmissible gametocyte states that are superior to those of the current clinical artemisinins and indeed of methylene blue (47, 48). These thus have the potential to block transmission, the important TCP5 feature. A substantial advantage of the amino-artemisinins is that none generates DHA as a metabolite but, like the current clinical artemisinins, they do possess relatively short half-lives. The ultimate aim is to use one of these amino-artemisinins in combination with a redox-active drug and a third drug with a different mode of action, both of which possess substantially longer half-lives, in assembling new TACTs for treatment of malaria. In working toward this goal, we have already demonstrated that combinations of artemiside or artemisone with the redox drug methylene blue exert synergistic activity against transmissible-stage *P. falciparum* gametocytes (47). The high efficacy of methylene blue-based combinations strongly encourages further investigation into combinations involving the amino-artemisinins, redox compounds such as phenoxazines, naphthoquinones, and others, and a third drug with a different mode of action (48).

Conclusion. The amino-artemisinins present *in vitro* ADME and *in vivo* PK properties that are similar or improved compared to those of DHA and artemether. Although artemisone is readily metabolized to M1 as reflected in its low elimination half-life, it displays a greater bioavailability (Table 3) that likely is due to improved solubility (Table 1). Its principal metabolite M1 is also soluble, has a much greater microsomal half-life than artemisone, and is highly active against *P. falciparum in vitro*. Although artemiside has low aqueous solubility, its potency against all *P. falciparum* blood stages, its synergism with methylene blue against transmissible blood-stage parasites (47), and its metabolism to artemisone (and thence the metabolite M1) also favor its continued examination. Of the others, the sulfamide is relatively soluble and, uniquely for an artemisinin, possesses good stability and bioavailability. While the arylurea has inferior solubility and bioavailability, it is easily prepared (48), has relatively low toxicity, and is highly potent against all *P. falciparum* blood stages. 11-Aza-artemisinin displays good solubility and metabolic stability, but it does have lower efficacy. However, its derivatives are substantially more active against *P. falciparum* (61, 62) and the apicomplexan parasite *Neospora caninum* (84), and this aspect coupled with the favorable PK data of the parent encourages their further examination.

MATERIALS AND METHODS

Ethics. All studies and procedures were conducted with prior approval of the animal ethics committee of the University of Cape Town (approval number 013/028) in accordance with the South African

National Standards (SANS 10386:2008) for the Care and Use of Animals for Scientific Purposes (85) and guidelines from the Department of Health (86). The use of human plasma was approved by the human research ethics committee of the University of Cape Town (HREC 783/2016).

Materials. Preparation of the amino-artemisinins 5 to 10 and 11-aza-artemisinin 11 and assessment of purity are described elsewhere (47, 48, 51, 52, 62). The artemisone metabolite M1 12 was prepared, characterized, and purified as previously described (51). All compounds submitted for screening were ≥95% pure according to high-performance liquid chromatography (HPLC) analyses as previously described (48).

Human whole blood and human plasma were obtained from the Western Province blood transfusion services, Cape Town, South Africa. KH_2PO_4 and K_2HPO_4 were purchased from Merck (Darmstadt, Germany). Analytical-grade acetonitrile was purchased from Anatech (Johannesburg, South Africa). Analytical-grade dimethyl sulfoxide (DMSO), formic acid, carbamazepine, propranolol hydrochloride, warfarin, procaine hydrochloride, and vinpocetine were obtained from Sigma-Aldrich (St. Louis, MO, USA). NADPH was purchased from Sigma-Aldrich (Steinheim, Germany). Polyethylene glycol (PEG), polypropylene glycol (PPG), and hydroxypropylmethylcellulose (HPMC) were purchased from Sigma-Aldrich (St. Louis, MO, USA). Human, rat, and mouse liver microsomes were obtained from Xenotech (KS, USA). All other reagents were of bioanalytical grade. Water was purified via a Milli-Q purification system (Millipore, Bedford, MA, USA).

For kinetic solubility assays, three solutions with differing pH were prepared. Phosphate-buffered saline (PBS) was prepared by mixing KH_2PO_4 (0.2 g), K_2HPO_4 (0.115 g), NaCl (0.8 g), and KCl (0.2 mg) in purified water (100 ml). The pH was measured and adjusted using 0.05 M HCl or 0.05 M NaOH to pH 7.4. The pH 2 solution was prepared by adding HCl (37%, 83 μl) to purified water (50 ml). FaSSIF buffer at pH 6.5 was prepared by adding KH_2PO_4 (2.042 g) and KCl (3.728 g) to purified water (450 ml) and adjusting the pH to 6.5 using 0.05 M HCl or 0.05 M NaOH as required. Simulated intestinal fluid (SIF) (Biorelevant, London, UK) powder (5.6 mg) was then added to the buffer (25 ml) to complete the process.

For the liquid-liquid extraction of plasma samples, a universal buffer containing the internal standard at pH 8 was utilized. The universal buffer consists of a 1:1 mixture of buffer A comprising CH_3COOH (5.72 ml), H_3PO_4 (6.82 ml), and H_3BO_3 (6.183 g) in purified water (1 liter) and buffer B comprising NaOH (20 g) in purified water (1 liter).

ADME profiling *in vitro*. (i) Kinetic solubility. Duplicate stock solutions of each compound at a concentration of 10 mM in DMSO were prepared in a 96-well plate in PBS at pH 7.4, water at pH 2, and FaSSIF buffer at pH 6.5 to a final concentration of 200 μM (68). These three solutions mimic the pH and conditions of the gastrointestinal tract. As the FaSSIF buffer mimics the fasted state *in vitro*, solubility in this buffer provides a guide as to whether compounds should be dosed with or without meals (87). Calibration standards were prepared for each compound in DMSO at 11, 100, and 220 μM. These standards were used to produce a calibration curve required for calculation of the concentration of each compound in the test solutions. The exception was 11-aza-artemisinin, which proved to be less soluble in DMSO in initial kinetic solubility studies, but it did dissolve in the polar test solutions. The assay was repeated with calibration standards prepared in methanol, and as the standards were within acceptable ranges, the results were considered reliable. Plates were agitated on a plate shaker for 2 h (500 rpm, 22°C). Sample analysis was carried out by liquid chromatography-tandem mass spectrometry (LC-MS/MS) analysis as described in "Sample analysis" below. Peak areas were integrated, and calibration curves were constructed and used to calculate the concentrations of each compound in the three buffers.

(ii) Metabolic stability in liver microsomes. The metabolic stability assay was performed in duplicate using 96-deepwell plates. Each compound (0.4 mM) was incubated individually in mouse, rat, and pooled human liver microsomes (0.4 mg/ml) at 37°C in the presence and absence of the cofactor NADPH (1 mM). An aliquot was taken at 0, 5, 10, 30, and 60 min, and the reaction was quenched by adding 300 μl of ice-cold acetonitrile containing the internal standard carbamazepine (0.0236 μg/ml) (88). The test compounds in the supernatant were analyzed by means of LC-MS/MS as described in "Sample analysis" below. The normalized data for each sample were used to calculate the *in vitro* half-life, intrinsic clearance rate, and hepatic extraction ratio from the results of this assay using the following equations (88).

Equation 1. Normalized area.

$$\text{Normalized area} = \left(\frac{\text{Peak area of sample at time point}}{\text{Peak area of internal standard}}\right) \tag{1}$$

Equation 2. Percent parent remaining.

$$\%\ \text{Parent} = \frac{\text{Normalized peak area of sample at time point}}{\text{Normalized peak area of sample at } t = 0} \times 100 \tag{2}$$

Equation 3. Calculated $t_{1/2}$.

$$t_{1/2} = -0.693/\lambda \tag{3}$$

where λ is the slope of the ln (% parent remaining) versus time curve of the compound.

Equation 4. CL_{int}.

$$\text{CL}_{\text{int}} = \left[\frac{0.693}{t_{1/2}(\text{min})}\right] \times \left[\frac{\text{Volume of incubation } (\mu\text{l})}{\text{Microsomal protein } (\mu\text{g})}\right] \tag{4}$$

Equation 5. Hepatic extraction ratio.

$$E_H = \frac{f_u \times CL_{int}}{QH + f_u \times CL_{int}} \quad (5)$$

(iii) Plasma protein binding. Plasma protein binding was measured using an ultracentrifugation method. The assay was performed using a 96-well microtiter plate with pooled human plasma spiked with the test compound (10 μM). An aliquot was removed and quenched using ice-cold acetonitrile containing the internal standard carbamazepine (0.0236 μg/ml) and placed in the freezer. This served as the total concentration sample. After preincubation at 37°C for 1 h, duplicate aliquots of the spiked plasma were transferred to ultracentrifugation tubes and ultracentrifuged for 4 h (216,937 $\times$ *g*, 37°C, Beckman Optima L-80XP). Analyte concentration of all compounds and sample types were determined by means of LC-MS/MS as described in "Sample analysis" below.

Pharmacokinetics *in vivo*. (i) Animals. Healthy male C57/BL6 mice each weighing approximately 25 g were used. The mice maintained at the University of Cape Town animal facility were housed in 27 by 21 by 18 cm cages, under controlled environmental conditions at 22 $\pm$ 2°C and a 12-h light/dark cycle. Humidity was monitored and ranged between 55 and 70%. Food and water were available *ad libitum*. Mice were acclimatized to their environment for 7 days before experiments were initiated.

(ii) Oral drug administration. Each of artemether, the amino-artemisinins 5 to 10, and 11-aza-artemisinin 11 (12.5 mg) was dissolved in 0.2 ml DMSO, to which 1.8 ml 0.5% (wt/vol) HPMC in water was then added. Compounds were administered orally via gavage at a dose of 50 mg/kg ($n = 3$). Dosing volumes were calculated based on the weight of each mouse in the respective group. The dosing volumes ranged between 160 μl and 200 μl, ensuring that the dose remained at 50 mg/kg. Blood samples for amino-artemisinins 5 to 8 and 10 were collected via tail-bleeding predose and at 0.08, 0.25, 0.5, 1, 2, and 4 h. Blood samples for the phenylurea 9 and 11-aza-artemisinin 11 were collected at 0.08, 0.5, 1, 2, 4, 8, and 24 h postdose. Samples were placed in 0.5 ml lithium heparin micro vials to prevent blood coagulation. Artemether and the amino-artemisinins 5 to 8 and 10 were expected to display the characteristic short half-lives of the artemisinins, and therefore it was more important to map the initial exposure over 4 h. The phenylurea 9 and the 11-aza-artemisinin 11 were predicted to have longer half-lives and were sampled over a greater time period. The samples were immediately centrifuged at 5,590 $\times$ *g* for 5 min and the plasma was transferred to new microvials. The plasma samples were stored at −80°C.

(iii) Intravenous drug administration. For the intravenous formulations, each of artemether, the amino-artemisinins 5 to 10, and 11-aza-artemisinin 11 (2.5 mg) was dissolved in 1 ml DMSO/PEG/PPG (1:3:6, vol/vol). DMSO was added first, followed by PEG and then PPG. The resulting solutions in the mixture of DMSO, PEG, and PPG (1:3:6, vol/vol) were administered intravenously at a dose of 10 mg/kg ($n = 3$) via injection into the dorsal penile vein. Mice were anesthetized with an intraperitoneal injection of a saline ketamine/xylazine solution. This consisted of 1 ml ketamine (100 mg/ml), 0.5 ml xylazine (20 mg/ml), and 8.5 ml PBS solution to make a total volume of 10 ml. Dosage of anesthetic preparation for mice was 0.8 ml/10 g body weight; this amounts to a dose of 80 mg/kg ketamine and 10 mg/kg xylazine. The total volume of administration was dose adjusted to 10 mg/kg with an approximate volume of 80 μl, according to the weight of each animal on the morning of dosing. Blood samples for the amino-artemisinins 5 to 8 and 10 were collected via tail-bleeding predose and at 0.08, 0.25, 0.5, 1, 2, and 4 h, and blood samples for the phenylurea 9 and 11-aza-artemisinin 11 were collected at 0.08, 0.5, 1, 2, 4, 8, and 24 h postdose. Samples were all placed in 0.5 ml lithium heparin microvials to prevent blood coagulation. The samples were immediately centrifuged at 5,590 $\times$ *g* for 5 min and the plasma was transferred to new microvials. The plasma samples were stored at −80°C.

Sample analysis. Concentrations of the kinetic solubility, metabolic stability, plasma stability, plasma protein binding samples, and plasma samples from murine studies were determined using quantitative LC-MS/MS assays.

Sample extraction. For sample extraction from the kinetic solubility, metabolic stability, plasma stability, and plasma protein binding studies, each compound was extracted from 200 μl of acetonitrile by adding 350 μl ethyl acetate, which contained the internal standard carbamazepine, and vortexing for 1 min followed by centrifugation at 5,590 $\times$ *g* for 5 min. The organic layer was then transferred and evaporated under a gentle stream of nitrogen at room temperature for 30 min. The dried samples were reconstituted in mobile phase, and a 5 μl sample was injected for LC-MS/MS analysis. The only exception was the arylurea 10, for which no liquid-liquid extraction was conducted; instead, the 200 μl acetonitrile solution was evaporated under a gentle stream of nitrogen at room temperature. The dried sample was reconstituted in the mobile phase, and a 5 μl sample was injected for LC-MS/MS analysis. The plasma samples for each compound from the *in vivo* studies were extracted by mixing 350 μl ethyl acetate with 15 μl of plasma sample and 35 μl of universal buffer containing internal standard at pH 8. The samples were vortexed for 1 min and centrifuged for 5 min, and the organic layer was then transferred and evaporated under a gentle stream of nitrogen at room temperature for 30 min. The dried samples were each reconstituted in the mobile phase, and a 5 μl sample was injected for LC-MS/MS analysis.

LC-MS/MS analysis. For all the artemisinins except the arylurea 10, gradient chromatography was performed on a Phenomenex (Torrance, CA, USA) Luna PFP(2) analytical column (100 Å, 5 μm, 2 by 50 mm) and an AB Sciex API 5500 mass spectrometer which was operated at unit resolution in the multiple reaction monitoring (MRM) mode. The HPLC method used was a gradient method with 5 mM ammonium acetate and 0.1% acetic acid in water as the aqueous phase and a mixture of acetonitrile and methanol (1:1 vol/vol) containing 5% of the aqueous phase as the organic phase (89). The arylurea 10 was analyzed using a Phenomenex Gemini NX-C18 (5 μm, 2.1 mm by 50 mm) column with an AB Sciex 3200 QTRAP mass spectrometer operated at unit resolution in the MRM mode. The HPLC method used was a gradient method with 5 mM ammonium acetate and 0.1% acetic acid in water as the aqueous phase and a mixture of

acetonitrile and methanol (1:1 vol/vol). The transitions of the molecular ions were monitored, as listed in Table S8 in the supporting information. The calibration range was between 0.002 μg/ml and 6.250 μg/ml. Data acquisition and evaluation were performed using Analyst 1.6.2 software (Applied Biosystems, Foster City, CA, USA). The formation of the putative metabolite DHA from the amino-artemisinins and the metabolite M1 of artemisone were evaluated in these mice PK studies; the MRM transitions of DHA and M1 (Table S8) were thus included in the LC-MS/MS assays. Data for the artemether product ion are consistent with those presented elsewhere (35).

Data analysis. Drug concentration versus time plots for each compound were used to determine maximal drug concentration C_{max}, time T_{max} to reach C_{max}, elimination half-life $t_{1/2}$, and the area under the concentration-time curve from time zero to last, AUC_{0-last}. From these values, the PK parameters clearance (CL), volume of distribution (V), and oral bioavailability (F) could be determined using the noncompartmental analysis software PK Solutions version 2.0, Summit Research Services, Montrose, USA. The area under the plasma concentration curve up to the last time point AUC_{0-last} was calculated by using the trapezoidal rule (90).

SUPPLEMENTAL MATERIAL

Supplemental material is available online only.

SUPPLEMENTAL FILE 1, PDF file, 0.3 MB.

ACKNOWLEDGMENTS

This work was funded by the South African Medical Research Council (MRC) Flagship Project MALTB-Redox with funds from the National Treasury under its Economic Competitiveness and Support Package (UID MRC-RFA-UFSP-01-2013) and South African National Research Foundation grants to Richard K. Haynes (UIDs 90682 and 98934).

REFERENCES

1. World Health Organization. 2019. Geneva: world malaria report 2019.
2. Hamilton WL, Amato R, van der Pluijm RW, Jacob CG, Quang HH, Thuy-Nhien NT, Hien TT, Hongvanthong B, Chindavongsa K, Mayxay M, Huy R, Leang R, Huch C, Dysoley L, Amaratunga C, Suon S, Fairhurst RM, Tripura R, Peto TJ, Sovann Y, Jittamala P, Hanboonkunupakarn B, Pukrittayakamee S, Chau NH, Imwong M, Dhorda M, Vongpromek R, Chan XHS, Maude RJ, Pearson RD, Nguyen T, Rockett K, Drury E, Gonçalves S, White NJ, Day NP, Kwiatkowski DP, Dondorp AM, Miotto O. 2019. Evolution and expansion of multidrug resistant malaria in Southeast Asia: a genomic epidemiology study. Lancet Infect Dis 19:943–951. https://doi.org/10.1016/S1473-3099(19)30392-5.
3. Witmer K, Dahalan FA, Delves MJ, Yahiya S, Watson OJ, Straschil U, Chiwcharoen D, Sornboon B, Pukrittayakamee S, Pearson RD, Howick VM, Lawniczak MKN, White NJ, Dondorp AM, Okell LC, Chotivanich K, Ruecker A, Baum J. 2020. Transmission of artemisinin-resistant malaria parasites to mosquitoes under antimalarial drug pressure. Antimicrob Agents Chemother 65:e00898-20. https://doi.org/10.1128/AAC.00898-20.
4. MalariaGEN Plasmodium falciparum Community Project. 2016. Genomic epidemiology of artemisinin resistant malaria. Elife 5:e08714. https://doi.org/10.7554/eLife.08714.
5. Miotto O, Sekihara M, Tachibana S-I, Yamauchi M, Pearson RD, Amato R, Gonçalves S, Mehra S, Noviyanti R, Marfurt J, Auburn S, Price RN, Mueller I, Ikeda M, Mori T, Hirai M, Tavul L, Hetzel MW, Laman M, Barry AE, Ringwald P, Ohashi J, Hombhanje F, Kwiatkowski DP, Mita T. 2020. Emergence of artemisinin-resistant *Plasmodium falciparum* with *kelch13* C580Y mutations on the island of New Guinea. PLoS Pathog 16:e1009133. https://doi.org/10.1371/journal.ppat.1009133.
6. Ariey F, Witkowski B, Amaratunga C, Beghain J, Langlois A-C, Khim N, Kim S, Duru V, Bouchier C, Ma L, Lim P, Leang R, Duong S, Sreng S, Suon S, Chuor CM, Bout DM, Ménard S, Rogers WO, Genton B, Fandeur T, Miotto O, Ringwald P, Le Bras J, Berry A, Barale J-C, Fairhurst RM, Benoit-Vical F, Mercereau-Puijalon O, Ménard D. 2014. A molecular marker of artemisinin-resistant Plasmodium falciparum malaria. Nature 505:50–55. https://doi.org/10.1038/nature12876.
7. Takala-Harrison S, Jacob CG, Arze C, Cummings MP, Silva JC, Dondorp AM, Fukuda MM, Hien TT, Mayxay M, Noedl H, Nosten F, Kyaw MP, Nhien NTT, Imwong M, Bethell D, Se Y, Lon C, Tyner SD, Saunders DL, Ariey F, Mercereau-Puijalon O, Menard D, Newton PN, Khanthavong M, Hongvanthong B, Starzengruber P, Fuehrer H-P, Swoboda P, Khan WA, Phyo AP, Nyunt MM, Nyunt MH, Brown TS, Adams M, Pepin CS, Bailey J, Tan JC, Ferdig MT, Clark TG, Miotto O, MacInnis B, Kwiatkowski DP, White NJ, Ringwald P, Plowe CV. 2015. Independent emergence of artemisinin resistance mutations among Plasmodium falciparum in Southeast Asia. J Infect Dis 211:670–679. https://doi.org/10.1093/infdis/jiu491.
8. Miotto O, Amato R, Ashley EA, MacInnis B, Almagro-Garcia J, Amaratunga C, Lim P, Mead D, Oyola SO, Dhorda M, Imwong M, Woodrow C, Manske M, Stalker J, Drury E, Campino S, Amenga-Etego L, Thanh T-NN, Tran HT, Ringwald P, Bethell D, Nosten F, Phyo AP, Pukrittayakamee S, Chotivanich K, Chuor CM, Nguon C, Suon S, Sreng S, Newton PN, Mayxay M, Khanthavong M, Hongvanthong B, Htut Y, Han KT, Kyaw MP, Faiz MA, Fanello CI, Onyamboko M, Mokuolu OA, Jacob CG, Takala-Harrison S, Plowe CV, Day NP, Dondorp AM, Spencer CCA, McVean G, Fairhurst RM, White NJ, Kwiatkowski DP, et al. 2015. Genetic architecture of artemisinin-resistant Plasmodium falciparum. Nat Genet 47:226–234. https://doi.org/10.1038/ng.3189.
9. Spring MD, Lin JT, Manning JE, Vanachayangkul P, Somethy S, Bun R, Se Y, Chann S, Ittiverakul M, Sia-Ngam P, Kuntawunginn W, Arsanok M, Buathong N, Chaorattanakawee S, Gosi P, Ta-Aksorn W, Chanarat N, Sundrakes S, Kong N, Heng TK, Nou S, Teja-Isavadharm P, Pichyangkul S, Phann ST, Balasubramanian S, Juliano JJ, Meshnick SR, Chour CM, Prom S, Lanteri CA, Lon C, Saunders DL. 2015. Dihydroartemisinin-piperaquine failure associated with a triple mutant including kelch13 C580Y in Cambodia: an observational cohort study. Lancet Infect Dis 15:683–691. https://doi.org/10.1016/S1473-3099(15)70049-6.
10. Kheang ST, Sovannaroth S, Ek S, Chy S, Chhun P, Mao S, Nguon S, Lek DS, Menard D, Kak N. 2017. Prevalence of K13 mutation and day-3 positive parasitaemia in artemisinin-resistant malaria endemic area of Cambodia: a cross-sectional study. Malar J 16:372. https://doi.org/10.1186/s12936-017-2024-4.
11. Sá JM, Kaslow SR, Krause MA, Melendez-Muniz VA, Salzman RE, Kite WA, Zhang M, Moraes Barros RR, Mu J, Han PK, Mershon JP, Figan CE, Caleon RL, Rahman RS, Gibson TJ, Amaratunga C, Nishiguchi EP, Breglio KF, Engels TM, Velmurugan S, Ricklefs S, Straimer J, Gnädig NF, Deng B, Liu A, Diouf A, Miura K, Tullo GS, Eastman RT, Chakravarty S, James ER, Udenze K, Li S, Sturdevant DE, Gwadz RW, Porcella SF, Long CA, Fidock DA, Thomas ML, Fay MP, Sim BKL, Hoffman SL, Adams JH, Fairhurst RM, Su X-Z, Wellems TE. 2018. Artemisinin resistance phenotypes and K13 inheritance in a *Plasmodium falciparum* cross and *Aotus* model. Proc Natl Acad Sci U S A 115:12513–12518. https://doi.org/10.1073/pnas.1813386115.
12. Mbengue A, Bhattacharjee S, Pandharkar T, Liu H, Estiu G, Stahelin RV, Rizk SS, Njimoh DL, Ryan Y, Chotivanich K, Nguon C, Ghorbal M, Lopez-Rubio J-J, Pfrender M, Emrich S, Mohandas N, Dondorp AM, Wiest O, Haldar K. 2015. A molecular mechanism of artemisinin resistance in Plasmodium falciparum malaria. Nature 520:683–687. https://doi.org/10.1038/nature14412.
13. Van Hook AM. 2015. Antimalarial drugs inhibit PI3P production. Sci Signal 8:ec118. https://doi.org/10.1126/scisignal.aac4781.
14. Rogers WO, Sem R, Tero T, Chim P, Lim P, Muth S, Socheat D, Frédéric Ariey F, Wongsrichanalai C. 2009. Failure of artesunate-mefloquine combination therapy for uncomplicated *Plasmodium falciparum* malaria in southern Cambodia. Malar J 8:10. https://doi.org/10.1186/1475-2875-8-10.

15. Veiga MI, Dhingra SK, Henrich PP, Straimer J, Gnädig N, Uhlemann A-C, Martin RE, Lehane AM, Fidock DA. 2016. Globally prevalent PfMDR1 mutations modulate Plasmodium falciparum susceptibility to artemisinin-based combination therapies. Nat Commun 7:11553. https://doi.org/10.1038/ncomms11553.
16. Phyo AP, Ashley EA, Anderson TJC, Bozdech Z, Carrara VI, Sriprawat K, Nair S, White MM, Dziekan J, Ling C, Proux S, Konghahong K, Jeeyapant A, Woodrow CJ, Imwong M, McGready R, Lwin KM, Day NPJ, White NJ, Nosten F. 2016. Declining efficacy of artemisinin combination therapy against *P falciparum* malaria on the Thai-Myanmar border (2003–2013): the role of parasite genetic factors. Clin Infect Dis 63:784–791. https://doi.org/10.1093/cid/ciw388.
17. Phyo AP, von Seidlein L. 2017. Challenges to replace ACT as first-line drug. Malar J 16:296. https://doi.org/10.1186/s12936-017-1942-5.
18. Taylor SM, Juliano JJ. 2014. Artemisinin combination therapies and malaria parasite drug resistance: the game is afoot. J Infect Dis 210:335–337. https://doi.org/10.1093/infdis/jiu142.
19. World Health Organization, Geneva. Global malaria programme August 2018 status report information and data. http://www.who.int/malaria/areas/drug_resistance/en/
20. van der Pluijm RW, Tripura R, Hoglund RM, Phyo AP, Lek D, Ul Islam A, Anvikar AR, Satpathi P, et al. 2020. Triple artemisinin-based combination therapies versus artemisinin-based combination therapies for uncomplicated Plasmodium falciparum malaria: a multicentre, open-label, randomised clinical trial. Lancet https://doi.org/10.1016/S0140-6736(20)30552-3.
21. Haynes RK, Cheu KW, Chan HW, Wong HN, Li KY, Tang MMK, Chen M-J, Guo Z-F, Guo Z-H, Sinniah K, Witte AB, Coghi P, Monti D. 2012. Interactions between artemisinins and other antimalarial drugs in relation to the co-factor model – a unifying proposal for drug action. ChemMedChem 7:2204–2226. https://doi.org/10.1002/cmdc.201200383.
22. Krishna S. 2019. Triple artemisinin-containing combination anti-malarial treatments should be implemented now to delay the emergence of resistance: the case against. Malar J 18:339. https://doi.org/10.1186/s12936-019-2976-7.
23. Rosenthal PJ. 2020. Are three drugs for malaria better than two? Lancet https://doi.org/10.1016/S0140-6736(20)30560-2.
24. Landier J, Parker DM, Thu AM, Lwin KM, Delmas G, Nosten FH, for the Malaria Elimination Task Force Group. 2018. Effect of generalised access to early diagnosis and treatment and targeted mass drug administration on *Plasmodium falciparum* malaria in Eastern Myanmar: an observational study of a regional elimination programme. Lancet 391:1916–1926. https://doi.org/10.1016/S0140-6736(18)30792-X.
25. von Seidlein L, Peto TJ, Landier J, Nguyen T-N, Tripura R, Phommasone K, Pongvongsa T, Lwin KM, Keereecharoen L, Kajeechiwa L, Thwin MM, Parker DM, Wiladphaingern J, Nosten S, Proux S, Corbel V, Tuong-Vy N, Phuc-Nhi TL, Son DH, Huong-Thu PN, Tuyen NTK, Tien NT, Dong LT, Hue DV, Quang HH, Nguon C, Davoeung C, Rekol H, Adhikari B, Henriques G, Phongmany P, Suangkanarat P, Jeeyapant A, Vihokhern B, van der Pluijm RW, Lubell Y, White LJ, Aguas R, Promnarate C, Sirithiranont P, Malleret B, Rénia L, Onsjö C, Chan XH, Chalk J, Miotto O, Patumrat K, Chotivanich K, Hanboonkunupakarn B, Jittmala P, et al. 2019. The impact of targeted malaria elimination with mass drug administrations on falciparum malaria in Southeast Asia: a cluster randomised trial. PLoS Med 16:e1002745. https://doi.org/10.1371/journal.pmed.1002745.
26. Mendis K. 2019. Mass drug administration should be implemented as a tool to accelerate elimination: against. Malar J 18:279. https://doi.org/10.1186/s12936-019-2907-7.
27. Orive G, Lertxundi U. 2020. Mass drug administration: time to consider drug pollution? Lancet 395:1112–1113. https://doi.org/10.1016/S0140-6736(20)30053-2.
28. Kyaw SS, Delmas G, Drake TL, Celhay O, Pan-Ngum W, Pukrittayakamee S, Lubell Y, Aguas RJ, Maude RJ, White LJ, Nosten F. 2021. Estimating the programmatic cost of targeted mass drug administration for malaria in Myanmar. BMC Public Health 21:826. https://doi.org/10.1186/s12889-021-10842-5.
29. Ramos-Martín V, González-Martínez C, Mackenzie I, Schmutzhard J, Pace C, Lalloo DG, Terlouw DJ. 2014. Neuroauditory toxicity of artemisinin combination therapies—have safety concerns been addressed? Am J Trop Med Hyg 91:62–73. https://doi.org/10.4269/ajtmh.13-0702.
30. World Health Organization, Geneva. The Mekong Malaria Elimination Programme - countries of the Greater Mekong ready for the "last mile" of malaria elimination; bulletin no. 9. December 2020. https://www.who.int/publications/i/item/WHO-UCN-GMP-MME-2020.05.
31. Zhang JF. 2005. A detailed chronological record of project 523 and the discovery and development of Qinghaosu (Artemisinin). Yang Cheng Evening News Publishing Company, Yang Cheng, China.
32. Guoqiao L, Ying L, Zelin L, Meiyi Z (ed). 2018. Artemisinin-based and other antimalarials: detailed account of studies by Chinese scientists who discovered and developed them. Academic Press, Elsevier
33. Ma N, Zhang Z, Liao F, Jiang T, Tu Y. 2020. The birth of artemisinin. Pharmacol Ther 216:107658. https://doi.org/10.1016/j.pharmthera.2020.107658.
34. Xing J, Bai KH, Liu T, Wang RL, Zhang LF, Zhang SQ. 2011. The multiple-dosing pharmacokinetics of artemether, artesunate, and their metabolite dihydroartemisinin in rats. Xenobiotica 41:252–258. https://doi.org/10.3109/00498254.2010.542257.
35. Liu T, Du F, Zhu F, Xing J. 2011. Metabolite identification of artemether by data-dependent accurate mass spectrometric analysis using an LTQ-Orbitrap hybrid mass spectrometer in combination with the online hydrogen/deuterium exchange technique. Rapid Commun Mass Spectrom 25:3303–3313. https://doi.org/10.1002/rcm.5214.
36. Zang M, Zhu F, Zhao L, Yang A, Li X, Liu H, Xing J. 2014. The effect of UGTs polymorphism on the auto-induction phase II metabolism-mediated pharmacokinetics of dihydroartemisinin in healthy Chinese subjects after oral administration of a fixed combination of dihydroartemisinin-piperaquine. Malar J 13:478. https://doi.org/10.1186/1475-2875-13-478.
37. Wesche DL, DeCoster MA, Tortella FC, Brewer TG. 1994. Neurotoxicity of artemisinin analogs in vitro. Antimicrob Agents Chemother 38:1813–1819. https://doi.org/10.1128/aac.38.8.1813.
38. Haynes RK, Schmuck G. 2000. Establishment of an in vitro screening model for neurodegeneration induced by antimalarial drugs of the artemisinin-type. Neurotox Res 2:37–49.
39. Nontprasert A, Pukrittayakamee S, Nosten-Bertrand M, Vanijanonta S, White NJ. 2000. Studies of the neurotoxicity of oral artemisinin derivatives in mice. Am J Trop Med Hyg 62:409–412. https://doi.org/10.4269/ajtmh.2000.62.409.
40. Efferth T, Kaina B. 2010. Toxicity of the antimalarial artemisinin and its derivatives. Crit Rev Toxicol 40:405–421. https://doi.org/10.3109/10408441003610571.
41. Haynes RK, Chan H-W, Lung C-M, Ng N-C, Wong H-N, Shek LY, Williams ID, Cartwright A, Gomes MF. 2007. Artesunate and dihydroartemisinin (DHA): unusual decomposition products formed under mild conditions and comments on the fitness of DHA as an antimalarial drug. ChemMedChem 2:1448–1463. https://doi.org/10.1002/cmdc.200700064.
42. Jansen FH. 2010. The pharmaceutical death-ride of dihydroartemisinin. Malar J 9:212. https://doi.org/10.1186/1475-2875-9-212.
43. Parapini S, Olliaro P, Navaratnam V, Taramelli D, Basilico N. 2015. Stability of the antimalarial drug dihydroartemisinin under physiologically-relevant conditions: implications for clinical treatment, pharmacokinetic and in vitro assays. Antimicrob Agents Chemother 59:4046–4052. https://doi.org/10.1128/AAC.00183-15.
44. Haynes RK. 2006. From artemisinin to new artemisinin antimalarials: biosynthesis, extraction, old and new derivatives, stereochemistry and medicinal chemistry requirements. Curr Top Med Chem 6:509–537. https://doi.org/10.2174/156802606776743129.
45. Kotoni D, Piras M, Cabri W, Giorgi F, Mazzanti A, Pierini M, Quaglia M, Villani C, Gasparrini F. 2014. Thermodynamic and kinetic investigation of monoketo-aldehyde-peroxyhemiacetal (MKA), a stereolabile degradation product of dihydroartemisinin. RSC Adv 4:32847–32857. https://doi.org/10.1039/C4RA00879K.
46. Dalrymple DG. 2012. Medicines for Malaria Venture (MMV), Geneva, Artemisia annua, Artemisinin, ACTs and Malaria Control in Africa; Tradition, Science and Public Policy. Politics & Prose, Washington, DC.
47. Coertzen D, Reader J, van der Watt M, Nondaba SH, Gibhard L, Wiesner L, Smith P, D'Alessandro S, Taramelli D, Wong HN, du Preez JL, Wu RWK, Birkholtz L-M, Haynes RK. 2018. Artemisone and artemiside are potent panreactive antimalarial agents that also synergize redox imbalance in *Plasmodium falciparum* transmissible gametocyte stages. Antimicrob Agents Chemother 62:e02214-17. https://doi.org/10.1128/AAC.02214-17.
48. Wong HN, Padín-Irizarry V, van der Watt ME, Reader J, Liebenberg W, Wiesner L, Smith P, Eribez K, Winzeler EA, Kyle DE, Birkholtz L-M, Coertzen D, Haynes RK. 2020. Optimal 10-aminoartemisinins with potent transmission-blocking capabilities for new artemisinin combination therapies – activities against blood stage *P falciparum* Including *Pf*KI3 C580Y mutants and liver stage *P berghei* parasites. Front Chem 7:901. https://doi.org/10.3389/fchem.2019.00901.
49. Beteck RM, Seldon R, Coertzen D, van der Watt ME, Reader J, Mackenzie JS, Lamprecht DA, Abraham M, Eribez K, Müller J, Rui F, Zhu G, de Grano RV, Williams ID, Smit FJ, Steyn AJC, Winzeler EA, Hemphill A, Birkholtz L-M, Warner DF, N'Da DD, Haynes RK. 2018. Accessible and distinct decoquinate derivatives active against *Mycobacterium tuberculosis* and apicomplexan parasites. Commun Chem 1:62. https://doi.org/10.1038/s42004-018-0062-7.

50. Wu Y, Wu RWK, Cheu KW, Williams ID, Krishna S, Slavic K, Gravett AM, Liu WM, Wong HN, Haynes RK. 2016. Methylene homologues of artemisone: an unexpected structure–activity relationship and a possible implication for the design of C10-substituted artemisinins. ChemMedChem 11:1469–1479. https://doi.org/10.1002/cmdc.201600011.
51. Haynes RK, Fugmann B, Stetter J, Rieckmann K, Heilmann H-D, Chan H-W, Cheung M-K, Lam W-L, Wong H-N, Croft SL, Vivas L, Rattray L, Stewart L, Peters W, Robinson BL, Edstein MD, Kotecka B, Kyle DE, Beckermann B, Gerisch M, Radtke M, Schmuck G, Steinke W, Wollborn U, Schmeer K, Römer A. 2006. Artemisone - a highly active antimalarial drug of the artemisinin class. Angew Chem Int Ed Engl 45:2082–2088. https://doi.org/10.1002/anie.200503071.
52. Chan WC, Chan DHW, Lee KW, Tin WS, Wong HN, Haynes RK. 2018. Evaluation and optimization of synthetic routes from dihydroartemisinin to the alkylamino-artemisinins artemiside and artemisone: a test of N-glycosylation methodologies on a lipophilic peroxide. Tetrahedron 74:5156–5171. https://doi.org/10.1016/j.tet.2018.04.027.
53. Schmuck G, Temerowski M, Haynes RK, Fugmann B. 2003. Identification of non-neurotoxic artemisinin derivatives in vivo and in vitro. Res Adv Antimicrob Agents Chemother 3:35–47.
54. Nagelschmitz J, Voith B, Wensing G, Roemer A, Fugmann B, Haynes RK, Kotecka BM, Rieckmann KH, Edstein MD. 2008. First assessment in humans of the safety, tolerability, pharmacokinetics, and ex vivo pharmacodynamic antimalarial activity of the new artemisinin derivative artemisone. Antimicrob Agents Chemother 52:3085–3091. https://doi.org/10.1128/AAC.01585-07.
55. Waknine-Grinberg JH, Hunt N, Bentura-Marciano A, McQuillan JA, Chan H-W, Chan W-C, Barenholz Y, Haynes RK, Golenser J. 2010. Artemisone effective against murine cerebral malaria. Malar J 9:227. https://doi.org/10.1186/1475-2875-9-227.
56. Krudsood S, Wilairatana P, Chalermrut K, Leowattana W, Voith B, Hampel B, et al. 2005. Artemifone, a new anti-malarial artemisinin derivative: open pilot trial to investigate the antiparasitic activity of BAY 44-9585 in patients with uncomplicated *P. falciparum* malaria. *In* XVI international congress for tropical medicine and malaria: medicine and health in the tropics.
57. Tse EG, Korsik M, Todd MH. 2019. A phase II trial planned for Cambodia in 2009 was withdrawn for logistical reasons prevailing at the time, and not for other reasons as implied elsewhere. The past, present and future of anti-malarial medicines. Malar J 18:9. https://doi.org/10.1186/s12936-019-2724-z.
58. Nureye D, Salahaddin M, Zewudie A. 2020. Current medicines for malaria including resistance issues. J Pharmacol Pharmacother 11:90–99. https://doi.org/10.4103/jpp.JPP_23_20.
59. U.S. National Library of Medicine. Artemisone for the treatment of uncomplicated falciparum malaria in Western Cambodia (AMOS). https://clinicaltrials.gov/ct2/show/NCT00936767
60. Haynes RK, Chan H-W, Ho W-Y, Ko CK-F, Gerena L, Kyle DE, Peters W, Robinson BL. 2005. Convenient access both to highly antimalaria-active 10-arylaminoartemisinins, and to 10-alkyl ethers including artemether, arteether, and artelinate. Chembiochem 6:659–667. https://doi.org/10.1002/cbic.200400366.
61. Haynes RK, Wong H-N, Lee K-W, Lung C-M, Shek LY, Williams ID, Croft SL, Vivas L, Rattray L, Stewart L, Wong VK W, Ko BC B. 2007. Preparation of *N*-sulfonyl and -carbonyl-11-aza-artemisinins with greatly enhanced thermal stabilities: in vitro antimalarial activities. ChemMedChem 2:1464–1479. https://doi.org/10.1002/cmdc.200700065.
62. Harmse R, Coertzen D, Wong HN, Smit FJ, van der Watt ME, Reader J, Nondaba SH, Birkholtz L-M, Haynes RK, N'Da DD. 2017. Activities of 11-aza-artemisinin and *N*-sulfonyl derivatives against asexual and transmissible malaria parasites. ChemMedChem 12:2086–2093. https://doi.org/10.1002/cmdc.201700599.
63. Grobler L, Chavchich M, Haynes RK, Edstein MD, Grobler AF. 2014. Assessment of the induction of dormant ring stages in *Plasmodium falciparum* parasites by artemisone and artemisone entrapped in Pheroid vesicles *in vitro*. Antimicrob Agents Chemother 58:7579–7582. https://doi.org/10.1128/AAC.02707-14.
64. Hott A, Casandra D, Sparks KN, Morton LC, Castanares G-G, Rutter A, Kyle DE. 2015. Artemisinin-resistant Plasmodium falciparum parasites exhibit altered patterns of development in infected erythrocytes. Antimicrob Agents Chemother 59:3156–3167. https://doi.org/10.1128/AAC.00197-15.
65. Adjalley SH, Johnston GL, Li T, Eastman RT, Ekland EH, Eappen AG, Richman A, Sim BK, Lee MC, Hoffman SL, Fidock DA. 2011. Quantitative assessment of *Plasmodium falciparum* sexual development reveals potent transmission-blocking activity by methylene blue. Proc Natl Acad Sci U S A 108:1214–1223. https://doi.org/10.1073/pnas.1112037108.
66. Lanteri CA, Chaorattanakawee S, Lon C, Saunders DL, Rutvisuttinunt W, Yingyuen K, Bathurst I, Ding XC, Tyner SD. 2014. Ex vivo activity of endoperoxide antimalarials, including artemisone and arterolane, against multidrug-resistant *Plasmodium falciparum* isolates from Cambodia. Antimicrob Agents Chemother 58:5831–5840. https://doi.org/10.1128/AAC.02462-14.
67. White NJ. 1998. Preventing antimalarial drug resistance through combinations. Drug Resist Updat 1:3–9. https://doi.org/10.1016/S1368-7646(98)80208-2.
68. Kearns E, Di L. 2008. Drug-like properties: concepts, structure design and methods: from ADME to toxicity optimization, 1st ed. Academic Press.
69. Artemether: PubChem. https://pubchem.ncbi.nlm.nih.gov/compound/68911#section=Solubility.
70. Ansari MT, Hussain A, Nadeem S, Majeed H, Saeed-Ul-Hassan S, Tariq I, Mahmood Q, Khan AK, Murtaza G. 2015. Preparation and characterization of solid dispersions of artemether by freeze-dried method. Biomed Res Int 2015:109563. https://doi.org/10.1155/2015/109563.
71. Artemether: Drugbank; https://go.drugbank.com/drugs/DB06697.
72. Tan KR, Hwang J. 2018. Tafenoquine receives regulatory approval in USA for prophylaxis of malaria and radical cure of *Plasmodium vivax*. J Travel Med 25:tay071. https://doi.org/10.1093/jtm/tay071.
73. Melariri P, Kalombo L, Nkuna P, Dube A, Hayeshi R, Ogutu B, Gibhard L, deKock C, Smith P, Wiesner L, Swai H. 2015. Oral lipid-based nanoformulation of tafenoquine enhanced bioavailability and blood stage antimalarial efficacy and led to a reduction in human red blood cell loss in mice. Int J Nanomedicine 2015:1493–1503. https://doi.org/10.2147/IJN.S76317.
74. Mignani S, Rodrigues J, Tomas H, Jalal R, Singh PP, Majoral J-P, Vishwakarma RA. 2018. Present drug-likeness filters in medicinal chemistry during the hit and lead optimization process: how far can they be simplified? Drug Discov Today 23:605–615. https://doi.org/10.1016/j.drudis.2018.01.010.
75. van Agtmael M, Gupta V, van der Wösten TH, Rutten JPB, van Boxtel CJ. 1999. Grapefruit juice increases the bioavailability of artemether. Eur J Clin Pharmacol 55:405–410. https://doi.org/10.1007/s002280050648.
76. Stuchlíková LR, Matoušková P, Vokřál I, Lamka J, Szotáková B, Sečkařová A, Dimunová D, Nguyen LT, Várady M, Skálová L. 2018. Metabolism of albendazole, ricobendazole and flubendazole in *Haemonchus contortus* adults: sex differences, resistance-related differences and the identification of new metabolites. Int J Parasitol Drugs Drug Resist 8:50–58. https://doi.org/10.1016/j.ijpddr.2018.01.005.
77. Sokolova AY, Wyllie S, Patterson S, Oza SL, Read KD, Fairlamb AH. 2010. Cross-resistance to nitro drugs and implications for treatment of human African trypanosomiasis. Antimicrob Agents Chemother 54:2893–2900. https://doi.org/10.1128/AAC.00332-10.
78. Wyllie S, Patterson S, Stojanovski L, Simeons FRC, Norval S, Kime R, Read KD, Fairlamb AH. 2012. The anti-trypanosome drug fexinidazole shows potential for treating visceral leishmaniasis. Sci Transl Med 4:119re1. https://doi.org/10.1126/scitranslmed.3003326.
79. Vallès B, Coassolo P, Sousa GD, Aubert C, Rahman R. 1993. *In vitro* hepatic biotransformation of moclobemide (Ro 11–1163) in man and rat. Xenobiotica 23:1101–1111. https://doi.org/10.3109/00498259309059425.
80. Madani S, Howald WN, Lawrence RF, Shen DD. 2000. Analysis of hydroxylated and *N*-dealkylated metabolites of terfenadine in microsomal incubates by liquid chromatography–mass spectrometry. J Chromatogr B 741:145–153. https://doi.org/10.1016/S0378-4347(00)00042-6.
81. Nisar M, Wong LW-Y, Sung HH-Y, Haynes RK, Williams ID. 2018. Cocrystals of the antimalarial drug 11-azaartemisinin with three alkenoic acids of 1:1 or 2:1 stoichiometry. Acta Crystallogr C Struct Chem 74:742–751. https://doi.org/10.1107/S2053229618006320.
82. Harmse R, Wong HN, Smit F, Haynes RK, N'Da DD. 2015. The case for development of 11-aza-artemisinins for malaria. Curr Med Chem 22:3607–3630. https://doi.org/10.2174/0929867322666150729115752.
83. Burrows JN, Duparc S, Gutteridge WE, Hooft van Huijsduijnen R, Kaszubska W, Macintyre F, Mazzuri S, Möhrle JJ, Wells TNC. 2017. New developments in anti-malarial target candidate and product profiles. Malar J 16:26. https://doi.org/10.1186/s12936-016-1675-x.
84. Harmse R, Wong HN, Smit FJ, Müller J, Hemphill A, N'Da DD, Haynes RK. 2017. Activities of 11-azaartemisinin and *N*-sulfonyl derivatives against *Neospora caninum* and comparative cytotoxicities. ChemMedChem 12:2094–2098. https://doi.org/10.1002/cmdc.201700600.
85. South African Bureau of Standards. 2008. SANS 10386:2008, edition 1. South African National Standard: The Care and Use of Animals for Scientific Purposes. SABS Standards Division, Pretoria, South Africa.
86. Department of Health. 2015. Ethics in health research: principles, processes and structures, 2nd ed. Department of Health, Republic of South Africa, Pretoria, South Africa.
87. Klein S. 2010. The use of biorelevant dissolution media to forecast the in vivo performance of a drug. AAPS J 12:397–406. https://doi.org/10.1208/s12248-010-9203-3.

88. Obach RS. 1999. Prediction of human clearance of twenty-nine drugs from hepatic microsomal intrinsic clearance data: an examination of in vitro half-life approach and nonspecific binding to microsomes. Drug Metab Dispos 27:1350–1359.
89. Steyn JD, Wiesner L, Du Plessis LH, Grobler AF, Smith PJ, Chan W-C, Haynes RK, Kotzé AF. 2011. Absorption of the novel artemisinin derivatives artemisone and artemiside: potential application of Pheroid™ technology. Int J Pharm 414:260–266. https://doi.org/10.1016/j.ijpharm.2011.05.003.
90. Gibhard L, Pravin K, Abay E, Wilhelm A, Swart K, Lawrence N, Khoury R, van der Westhuizen J, Smith P, Wiesner L. 2016. In vitro and in vivo pharmacokinetics of aminoalkylated diarylpropanes NP085 and NP102. Antimicrob Agents Chemother 60:3065–3069. https://doi.org/10.1128/AAC.02104-15.